

Quasiparticle Excitations and Charge Transition Levels of Oxygen Vacancies in Hafnia

Manish Jain,^{1,2} James R. Chelikowsky,³ and Steven G. Louie^{1,2}

¹*Department of Physics, University of California, Berkeley, California 94720*

²*Materials Sciences Division, Lawrence Berkeley,
National Laboratory, Berkeley, California 94720*

³*Center for Computational Materials,
Institute for Computational Engineering and Sciences,
Departments of Physics and Chemical Engineering,
University of Texas, Austin, 78712*

(Dated: October 27, 2018)

Abstract

We calculate the quasiparticle defect states and charge transition levels of oxygen vacancies in monoclinic hafnia. The charge transition levels, although they are thermodynamic quantities, can be critically dependent on the band gap owing to localized defect states. These quasiparticle defect level effects are treated using the first principle GW approximation to the self energy. We show that the quality and reliability of the results may be evaluated by calculating the same transition level via two physical paths and that it is important to include the necessary electrostatic corrections in a supercell calculation. Contrary to many previous reports, the oxygen vacancies in monoclinic hafnia are found to be a positive U center, where U is the defect electron addition energy. We identify a physical partitioning of U in terms of an electronic and structural relaxation part.

PACS numbers: 73.40.Qv, 85.30.Tv, 61.72.jd

Hafnia has recently received much attention because of its many applications, in particular as high-dielectric gate material replacing silica in microelectronic devices. However, devices based on hafnia suffer from several problems such as voltage threshold instabilities [1] and flat band voltage shifts [2]. These problems are believed to be due to a high density of defects in the material in particular oxygen vacancies are believed to play an important role as electron traps.

There have been several theoretical studies on the structural and electronic properties of oxygen vacancies in monoclinic hafnia. In early studies, formation energies as well as defect levels were calculated within density functional theory (DFT) using the local density approximation [3] and the generalized gradient approximation (GGA) [4]. The onsite energy, U , for adding an additional electron to the defect was calculated and the vacancies were found to be negative U [5] centers within these approximations. In these studies, however, the defect levels in the gap could not be determined unambiguously, owing to the well-known problem of underestimation of band gaps using Kohn-Sham eigenvalues [6]. Later studies used hybrid functionals [7–9] to calculate the defect levels of oxygen vacancies in hafnia. These functionals, which were constructed to fix the band gap underestimation problem, found that the defect was no longer a negative U center [8]. Recently, there has been a higher level theory study [10] using a combined DFT and GW approach on these defects. These authors found a negative U behavior for the oxygen vacancy. The GW part of the study in Ref. [10] was, however restricted to a 24-atom super cell.

In this letter, we report a new study of the quasiparticle excitations and charge transition levels of oxygen vacancies in monoclinic hafnia. To insure the accuracy of the results, we computed the charge transition levels via two physical paths and took into account an important electrostatic correction that was not included in the previous studies. The defects are found to be positive U centers. Further, we develop a methodology to understand the defect charging energy. We use a combined approach [11] based on DFT and GW formalism [6]. This formalism corrects for the error incurred in calculating formation energy and charge transition levels within standard DFT. The calculations were done using large super cells with 96 atoms. Such large super cells are necessary to minimize any spurious defect-defect interactions from overlap of the defect state wave functions in neighboring super cells.

The formation energy of a defect in charge state q and at arbitrary ionic coordinates \vec{R}

and chemical potential μ , $E_q^f(\vec{R})[\mu]$, can be expressed as

$$E_q^f(\vec{R})[\mu] = E_q(\vec{R}) - E_{\text{ref}} + \mu q \quad (1)$$

where $E_q(\vec{R})$ is the total energy of the system in charge state q and ionic coordinates \vec{R} , and E_{ref} is the energy of a reference system with the same number of atoms as the charged system. We note that \vec{R} is an arbitrary configuration which needs not be the equilibrium configuration of the charge state q which we denote as \vec{R}_q . Charge transition level, $\varepsilon^{q/q-1}$, is defined as the value of the chemical potential at which the charge state of the defect changes from q to $q-1$ ($q/q-1$). Conventionally, one defines the charge transition level from the valence band maximum, E_v . It is defined as the chemical potential μ at which the formation energies of the q and $q-1$ defects are equal and can be written in terms of formation energies as:

$$\varepsilon^{q/q-1} = E_{q-1}^f(\vec{R}_{q-1})[\mu = E_v] - E_q^f(\vec{R}_q)[\mu = E_v] \quad (2)$$

Within standard DFT, charge transition level is determined by calculating each of the formation energies in Eq. 2 in their respective equilibrium configurations as accurately as possible. But, because of the band gap problem and self-interaction terms within standard DFT methods, significant errors may be introduced. However, within the combined DFT and GW formalism, a charge transition level is written as:

$$\begin{aligned} \varepsilon^{q/q-1} &= [E_{q-1}^f(\vec{R}_{q-1}) - E_{q-1}^f(\vec{R}_q)] + [E_{q-1}^f(\vec{R}_q) - E_q^f(\vec{R}_q)] \\ &\equiv E_{\text{relax}} + E_{\text{QP}} \end{aligned} \quad (3)$$

by adding and subtracting the term $E_{q-1}^f(\vec{R}_q)$ [11]. (All the formation energies in the above expression as well as throughout the rest of the letter are evaluated with $\mu = E_v$.) This reformulation allows us to combine terms to eliminate most of the errors mentioned above. Figure 1 shows schematically the procedure for calculation of charge transition levels within the DFT+GW formalism. The first bracketed term on the right hand side of the Eq. 3 is a relaxation energy E_{relax} (red line in Figure 1) and the second bracketed term is a quasiparticle excitation energy E_{QP} (blue line in Figure 1). For the excitation energy, one uses the GW formalism [6]; while for the relaxation energy, one uses DFT. This ensures an accurate calculation of the appropriate physical quantities and hence the charge transition level and relative formation energies.

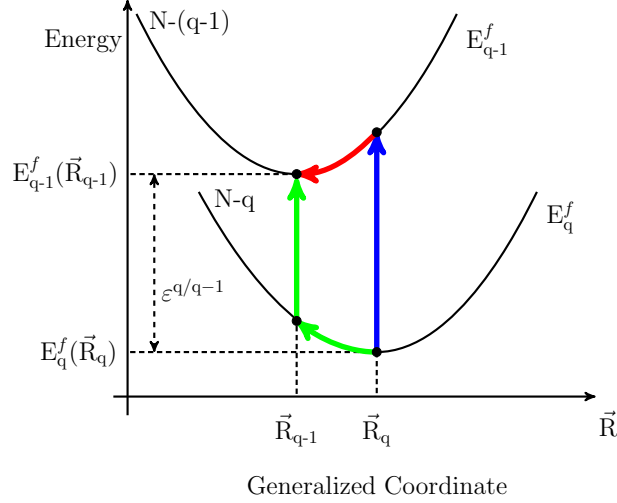


FIG. 1. Formation energies evaluated with $\mu = E_v$ vs. generalized coordinate, illustrating the terms in the DFT+GW formalism for the charge transition level $\varepsilon^{q/q-1}$

It is worth noting that the charge transition level is a thermodynamic quantity and does not depend on the path in the formation energy-generalized coordinate space one takes to calculate it. In other words, the value of charge transition level remains unaffected when one adds and subtracts any formation energy to it. In particular, we can alternatively choose to add and subtract $E_q^f(\vec{R}_{q-1})$ in Eq. 2. This would correspond to another path (the green line) in Figure 1. Calculating the charge transition level via multiple paths not only serves as a check for our calculations, but also gives some idea about the accuracy of the method.

For the DFT part of our calculation we used an *ab initio* pseudopotential plane-wave method, as implemented in QUANTUM ESPRESSO [12], with PBE [13] exchange correlation functional. We used non-local pseudopotentials constructed using the Troullier Martins [14] scheme with valence configurations $5s^25p^65d^26s^2$ and $2s^22p^4$ for Hf and O, respectively. The electronic wave functions were expanded in plane waves with cutoff energy of 250 Ry. The k-point sampling was restricted to the Γ point in view of the large super cell used. Our calculated lattice parameters for monoclinic hafnia are in excellent agreement with experiment [15] as well as with previous calculations [4]. Using the PBE eigenvalues and eigenfunctions, the quasiparticle energies were calculated within the G_0W_0 approximation [6] to the electron self-energy as implemented in the BerkeleyGW package [16]. The static dielectric matrix was calculated with a 10 Ry energy cutoff in a plane wave basis and extended to finite frequencies within the generalized plasmon pole model [6]. The band gap for

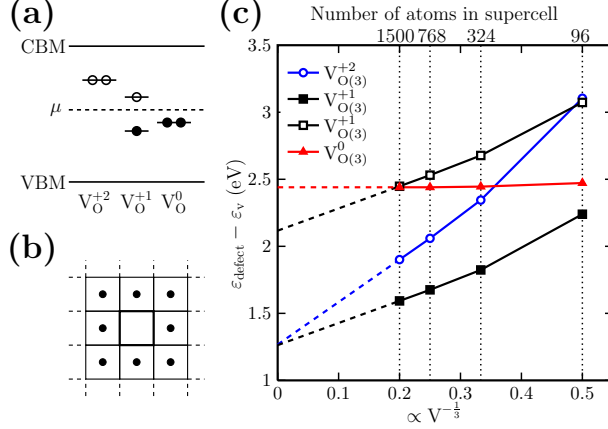


FIG. 2. (a) Schematic diagram showing both three and four fold coordinated oxygen vacancy induced defect levels in the band gap of hafnia for various charge states. (b) Periodic images of charged defects leading to a spurious electrostatic potential on the defect. (c) Effect of this spurious potential on eigenvalues. The plot shows cell size vs PBE eigenvalue with respect to the top of the valence band for vacancy induced defect states in V_{O_3} . The dashed line is the linear extrapolation to infinite super cell size.

bulk monoclinic hafnia is calculated to be 6.0 eV, which is in good agreement with previous studies 5.45-5.9 [10, 17] as well as experiments 5.7-5.9 [18, 19].

There are two distinct types of oxygen vacancies (with different coordination) in monoclinic hafnia – 3-fold coordinated (V_{O_3}) and 4-fold coordinated (V_{O_4}). We performed calculations for charge states $q = 0, 1, 2$ for both kind of vacancies, *i.e.* zero, one and two missing electrons from the vacancy.

Figure 2 (a) shows a schematic of the oxygen vacancy induced quasiparticle defect levels in the band gap of hafnia. The defect levels for all the charge states lie deep in the gap. Table I shows the relaxation energies (E_{relax}), quasiparticle energies (E_{QP}) and charge transition levels ($\epsilon^{q/q-1}$) calculated within DFT+GW approach. Despite the large differences in the quasiparticle energies required for the calculation in the two paths, the final charge transition levels via the two paths are always within 0.2 eV of one another. This gives us an error estimate of ± 0.1 eV for the DFT+GW method for calculation of charge transition levels.

It is worth noting that quasiparticle energies in Table I include an electrostatic correction owing to the super cell geometry used. Within the standard DFT-only methodology of calculating charge transition levels, one corrects the total energies of charged defects for

	V_{O_3}				V_{O_4}			
	+2/+1		+1/0		+2/+1		+1/0	
	P1	P2	P1	P2	P1	P2	P1	P2
E_{relax}	-0.64	0.76	-0.57	0.67	-0.75	0.80	-0.55	0.65
E_{QP}	3.30	1.69	3.93	2.88	3.04	1.33	3.46	2.50
$\varepsilon^{q/q-1}$	2.66	2.45	3.36	3.55	2.29	2.13	2.91	3.15
Avg. $\varepsilon^{q/q-1}$	2.56		3.46		2.21		3.03	

TABLE I. Table showing the two components contributing to the charge transition levels for V_{O_3} and V_{O_4} calculated within the DFT+GW methodology. P1 (P2) refers to Path 1 (2). Row 1 shows the relaxation energy (E_{relax}), Row 2 the quasiparticle energy (E_{QP}), Row 3 the charge transition level ($\varepsilon^{q/q-1}$) and Row 4 the value for $\varepsilon^{q/q-1}$ averaged over both paths. All values are in eV.

unphysical electrostatic terms from the charge on the image defects using Makov-Payne [20] like corrections. Within the DFT+GW method, the electrostatic error in the DFT eigenvalues in general needs to be accounted for. The origin of these electrostatic errors in the DFT eigenvalues is the spurious electrostatic potential from charged neighboring defects [21] as shown schematically in Figure 2 (b). To quantify these errors, we plotted the position of the Kohn-Sham defect level with respect to the valence band maximum for various super cell sizes as shown in Figure 2 (c). These calculations were done using the SIESTA code [22] with increasing super cell sizes - the largest of which contained 1499 atoms + defect. To get the infinite cell size value, we linearly extrapolated from the largest two super cell sizes. Figure 2 (c) shows that even at 1500 atoms, the errors are large with respect to the converged answer. Table II shows the effect of electrostatic corrections on quasiparticle defect levels along the two paths for V_{O_3} . The two paths have different electrostatic corrections to the quasiparticle energies and that these corrections are substantial. Accounting for these errors is important to get a reliable value of charge transition level.

Our quasiparticle defect levels and charge transition levels are in disagreement with previous DFT+GW calculations [10]. This disagreement is likely a consequence of their choice of a small super cell and, more importantly, neglect of electrostatic corrections. Reference [10]’s value of $\varepsilon^{+2/+1}$ for V_{O_3} (V_{O_4}) is 4.00 eV (3.22 eV) and of $\varepsilon^{+1/0}$ is 3.10 eV (2.43 eV); these values are close to our corresponding *uncorrected* values. Our calculations also dis-

	+2/+1		+1/0	
	P1	P2	P1	P2
E_{QP} (Uncorrected)	5.14	2.66	4.90	2.88
E_{QP} (Corrected)	3.30	1.69	3.93	2.88
ΔE_{QP}	1.84	0.97	0.97	0.00

TABLE II. Table showing effect of spurious charged super cell electrostatic corrections on the quasiparticle defect levels for V_{O_3} (referred to the top of the valence band). P1 (P2) refers to Path 1 (2). Row 1 shows the uncorrected quasiparticle energy, Row 2 the corrected quasiparticle energy, Row 3 the correction. All values are in eV.

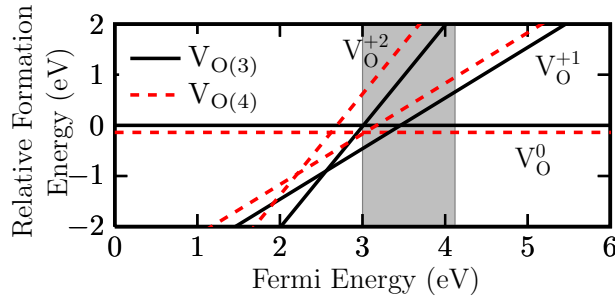


FIG. 3. Relative formation energy vs. chemical potential for charged oxygen vacancies in monoclinic hafnia. The shaded region denoted the Si band gap. The formation energy of $V_{O_4}^0$ is lower than $V_{O_3}^0$ by 0.14 eV.

agree with the hybrid functional value [8] of 3.7 eV for $\epsilon^{+2/+1}$ in V_{O_3} and 4.0 eV for $\epsilon^{+1/0}$ between $V_{O_3}^{+1}$ and $V_{O_4}^0$. (Our corresponding values are 2.56 eV and 3.32 eV respectively.) It is also worth noting that the Kohn-Sham eigenvalues calculated with hybrid functionals also disagree with our calculations. Also, in hybrid calculations, even though total energies were corrected for electrostatic errors, the eigenvalues were not. While this is not necessary for the charge transition level calculated as a total energy difference, it can lead to erroneous results whenever eigenvalues are directly compared to single-particle excitation experiment.

Figure 3 shows the relative formation energy of various charge states for the oxygen vacancies as a function of the chemical potential in monoclinic hafnia based on the values in Table I. The formation energy in Figure 3 is plotted with respect to the formation energy of $V_{O_3}^0$. As evident from Figure 3, $V_{O_3}^{+2}$, $V_{O_3}^{+1}$ and $V_{O_4}^0$ are the most stable defects in the system

depending on the value of μ . The experimentally relevant charge transition levels, $\varepsilon^{+2/+1}$ and $\varepsilon^{+1/0}$ would be 2.56 eV and 3.32 eV respectively. Not shown in the figure is the stability for V_O^{-1}/V_O^{-2} defects. For larger values of the chemical potential, the V_O^{-1}/V_O^{-2} defects may become more stable. Also, shown in Figure 3 (in shaded grey), is the band gap and the expected band offset for Si (~ 3 eV) when placed next to hafnia [19]. For p-doped Si next to hafnia, the system is expected to have $V_{O_3}^{+1}$ vacancies.

It is also noted from Figure 3 that oxygen vacancies are positive U centers. U is defined as the energy of the reaction: $2V^{+1} \rightarrow V^{2+} + V^0$. In terms of the charge transition levels, U for V^{+1} can be written as:

$$\begin{aligned} U &= E_{+2}^f(\vec{R}_{+2}) + E_0^f(\vec{R}_0) - 2E_{+1}^f(\vec{R}_{+1}) \\ &= -\varepsilon^{+2/+1} + \varepsilon^{+1/0} \end{aligned} \quad (4)$$

Our calculated values of U for both vacancies ($V_{O_3}^{+1}$ and $V_{O_4}^{+1}$) are given in Table III. Further, U can be broken into two parts – an electronic part (U_{elec}) and a relaxation part (U_{relax}) as defined in the curly brackets in the Eq. 5 below:

$$\begin{aligned} U &= \{E_{+2}^f(\vec{R}_{+1}) + E_0^f(\vec{R}_{+1}) - 2E_{+1}^f(\vec{R}_{+1})\} + \\ &\quad \{[E_{+2}^f(\vec{R}_{+2}) - E_{+2}^f(\vec{R}_{+1})] + [E_0^f(\vec{R}_0) - E_0^f(\vec{R}_{+1})]\} \\ &\equiv U_{\text{elec}} + U_{\text{relax}} \end{aligned} \quad (5)$$

This partitioning of U is instructive, because physically, U_{elec} represents the quasiparticle gap of the system in the +1 charge state keeping the structure fixed and U_{relax} represents sum of structural relaxation energies. Physically, $U_{\text{elec}} \geq 0$ and $U_{\text{relax}} \leq 0$. Table III shows our calculated values of U_{relax} and U_{elec} . The reason for large relaxation energy is that, in the +1 and +2 charge state, the atoms nearest to the vacancy relax by up to 5-10% of their bond lengths. This is in agreement with previous studies of relaxation around the vacancies [3, 4].

In conclusion, we have reported quasiparticle energies and charge transition levels of oxygen vacancies in monoclinic hafnia. We find that $V_{O_3}^{+2}$, $V_{O_3}^{+1}$ and $V_{O_4}^0$ are the most stable oxygen vacancies in the system as the Fermi level spans the band gap. By calculating the charge transition levels via two paths in configuration-space we gain insight to the charge defect stability and highlighted the importance of electrostatic corrections in super cell defect calculations. Further, we developed an intuitive partitioning of the defect charging energy U

	U_{elec}	U_{relax}	U_{total}
$V_{\text{O}_3}^{+1}$	2.24	-1.33	0.90
$V_{\text{O}_4}^{+1}$	2.13	-1.35	0.81

TABLE III. U for $V_{\text{O}_3}^{+1}$ and $V_{\text{O}_4}^{+1}$ calculated using the charge transition levels from Table I. Also shown are the contributions to U from electronic and relaxation components.

into a quasiparticle gap and sum of relaxation energies. Contrary to some previous studies, which found negative U or U close to zero, the oxygen vacancies were found to be positive U centers.

M.J. would like to thank Brad Malone and Dr. Georgy Samsonidze for fruitful discussions. This work was supported by National Science Foundation Grant No. DMR07-05941, the U.S. Department of Energy under Contract No. DE-AC02-05CH11231 and de-sc0001878. Computational resources have been provided by NSF through TeraGrid resources at NICS. M.J. was supported by the DOE. Part of the modeling and simulations were carried out with electronic structure and quasiparticle codes developed under NSF support.

-
- [1] G. Ribes, J. Mitard, M. Denais, S. Bruyere, F. Monsieur, C. Parthasarathy, E. Vincent, and G. Ghibaudo, *IEEE Trans. Device Mater. Reliab.* **5**, 5 (2005).
- [2] C. Hobbs *et al.*, *IEEE Trans. Electron Devices* **51**, 971 (2004).
- [3] A. S. Foster, F. Lopez Gejo, A. L. Shluger, and R. M. Nieminen, *Phys. Rev. B* **65**, 174117 (2002).
- [4] J. X. Zheng, G. Ceder, T. Maxisch, W. K. Chim, and W. K. Choi, *Phys. Rev. B* **75**, 104112 (2007); J. Kang, E.-C. Lee, and K. J. Chang, *Phys. Rev. B* **68**, 054106 (2003).
- [5] P. W. Anderson, *Phys. Rev. Lett.* **34**, 953 (1975).
- [6] M. S. Hybertsen and S. G. Louie, *Phys. Rev. B* **34**, 5390 (1986).
- [7] J. L. Gavartin, D. M. Ramo, A. L. Shluger, G. Bersuker, and B. H. Lee, *Appl. Phys. Lett.* **89**, 082908 (2006).
- [8] P. Broqvist and A. Pasquarello, *Appl. Phys. Lett.* **89**, 262904 (2006).
- [9] K. Xiong, J. Robertson, M. C. Gibson, and S. J. Clark, *Appl. Phys. Lett.* **87**, 183505 (2005).

- [10] E.-A. Choi and K. J. Chang, *Appl. Phys. Lett.* **94**, 122901 (2009).
- [11] M. Hedström, A. Schindlmayr, G. Schwarz, and M. Scheffler, *Phys. Rev. Lett.* **97**, 226401 (2006); P. Rinke, A. Janotti, M. Scheffler, and C. G. Van de Walle, *Phys. Rev. Lett.* **102**, 026402 (2009).
- [12] P. Giannozzi *et al.*, *J. Phys.: Condens. Matt.* **21**, 395502 (2009).
- [13] J. P. Perdew, K. Burke, and M. Ernzerhof, *Phys. Rev. Lett.* **77**, 3865 (1996).
- [14] N. Troullier and J. L. Martins, *Phys. Rev. B* **43**, 1993 (1991).
- [15] J. Wang, H. P. Li, and R. Stevens, *J. Mater. Sci.* **27**, 5397 (1992); D. M. Adams, S. Leonard, D. R. Russell, and R. J. Cernik, *J. Phys. Chem. Solids* **52**, 1181 (1991); D. W. Stacy, J. K. Johnstone, and D. R. Wilder, *J. Am. Ceram. Soc.* **55**, 482 (1972).
- [16] <http://www.berkeleygw.org>.
- [17] H. Jiang, R. I. Gomez-Abal, P. Rinke, and M. Scheffler, *Phys. Rev. B* **81**, 085119 (2010); M. Grüning, R. Shaltaf, and G.-M. Rignanese, *Phys. Rev. B* **81**, 035330 (2010).
- [18] S. Sayan, T. Emge, E. Garfunkel, X. Zhao, L. Wielunski, R. A. Bartynski, D. Vanderbilt, J. S. Suehle, S. Suzer, and M. Banaszak-Holl, *J. of Appl. Phys.* **96**, 7485 (2004).
- [19] E. Bersch, S. Rangan, R. A. Bartynski, E. Garfunkel, and E. Vescovo, *Phys. Rev. B* **78**, 085114 (2008).
- [20] G. Makov and M. C. Payne, *Phys. Rev. B* **51**, 4014 (1995).
- [21] S. Lany and A. Zunger, *Phys. Rev. B* **81**, 113201 (2010); C. Freysoldt, J. Neugebauer, and C. G. Van de Walle, *Phys. Rev. Lett.* **102**, 016402 (2009).
- [22] P. Ordejón, E. Artacho, and J. M. Soler, *Phys. Rev. B* **53**, R10441 (1996); J. M. Soler, E. Artacho, J. D. Gale, A. Garcia, J. Junquera, P. Ordejon, and D. Sanchez-Portal, *J. Phys.: Condens. Matt.* **14**, 2745 (2002).